

## Article

# Enhancing Inter-Patient Performance for Arrhythmia Classification with Adversarial Learning Using Beat-Score Maps

Yeqi Jeong , Jaewon Lee  and Miyoung Shin  \*

Bio-Intelligence & Data Mining Laboratory, Electronic and Electrical Engineering, Kyungpook National University, Daegu 41566, Republic of Korea; yeji7102@naver.com (Y.J.); realjaewon94@gmail.com (J.L.)

\* Correspondence: shinmy@knu.ac.kr; Tel.: +82-53-950-7562

**Abstract:** Research on computer-aided arrhythmia classification is actively conducted, but the limited generalization capacity constrains its applicability in practical clinical settings. One of the primary challenges in deploying such techniques in real-world scenarios is the inter-patient variability and the consequent performance degradation. In this study, we leverage our previous innovation, the n-beat-score map (n-BSM), to introduce an adversarial framework to mitigate the issue of poor performance in arrhythmia classification within the inter-patient paradigm. The n-BSM is a 2D representation of the ECG signal, capturing its constituent beat characteristics through beat-score vectors derived from a pre-trained beat classifier. We employ adversarial learning to eliminate patient-dependent features during the training of the beat classifier, thereby generating the patient-independent n-BSM (PI-BSM). This approach enables us to concentrate primarily on the learning characteristics associated with beat type rather than patient-specific features. Through a beat classifier pre-trained with adversarial learning, a series of beat-score vectors are generated for the beat segments that make up a given ECG signal. These vectors are then concatenated chronologically to form a PI-BSM. Utilizing PI-BSMs as the input, an arrhythmia classifier is trained to differentiate between distinct types of rhythms. This approach yields a 14.27% enhancement in the F1-score in the MIT-BIH arrhythmia database and a 4.97% improvement in cross-database evaluation using the Chapman–Shaoxing 12-lead ECG database.



**Citation:** Jeong, Y.; Lee, J.; Shin, M. Enhancing Inter-Patient Performance for Arrhythmia Classification with Adversarial Learning Using Beat-Score Maps. *Appl. Sci.* **2024**, *14*, 7227. <https://doi.org/10.3390/app14167227>

Academic Editor: Douglas O’Shaughnessy

Received: 5 July 2024

Revised: 1 August 2024

Accepted: 14 August 2024

Published: 16 August 2024



**Copyright:** © 2024 by the authors. Licensee MDPI, Basel, Switzerland. This article is an open access article distributed under the terms and conditions of the Creative Commons Attribution (CC BY) license (<https://creativecommons.org/licenses/by/4.0/>).

**Keywords:** arrhythmia classification; ECG individual differences; inter-patient scheme; adversarial learning

## 1. Introduction

Arrhythmia is one of the primary conditions of cardiovascular disease, which manifests as irregular heartbeats [1]. Depending on its specific type, it can swiftly lead to severe cardiac conditions [2,3]. Even non-life-threatening types of arrhythmias may progress to cardiovascular complications if left untreated [4]. In recent years, research on automatic arrhythmia classification using electrocardiogram (ECG) is actively underway [5]. However, only 10.4% of arrhythmia studies utilized an inter-patient scheme to consider real-world scenarios that reflect inter-patient variability in ECGs [6,7].

There are two paradigms for evaluating the performance of computer-assisted arrhythmia classification, namely inter-patient and intra-patient. Figure 1a depicts an inter-patient scheme, where the separation between the training and test sets is based on a subject-by-subject basis. Conversely, in the intra-patient scheme, as Figure 1b illustrates, the training and test set samples are collected without distinguishing between patients. Thus, the samples in both sets originate from the same individual.

According to [6], only 7.56% of studies exclusively addressed the inter-patient paradigm, while 89.4% considered only intra-patient schemes. Among the 11 studies utilizing both evaluation paradigms, the average classification accuracy within the intra-patient scheme stood at 98.39%, whereas it reached only 90.15% in the inter-patient scheme. This discrepancy arises from the substantial variation observed in ECG signals [8]. Notable differences

exist in the morphological and temporal properties of ECG signals between patients [9]. Even when patients share the same type of arrhythmia, the ECG signals may exhibit distinct characteristics. Moreover, the inter-patient scheme is preferable in realistic scenarios, albeit presenting challenges in overall classification performance degradation.

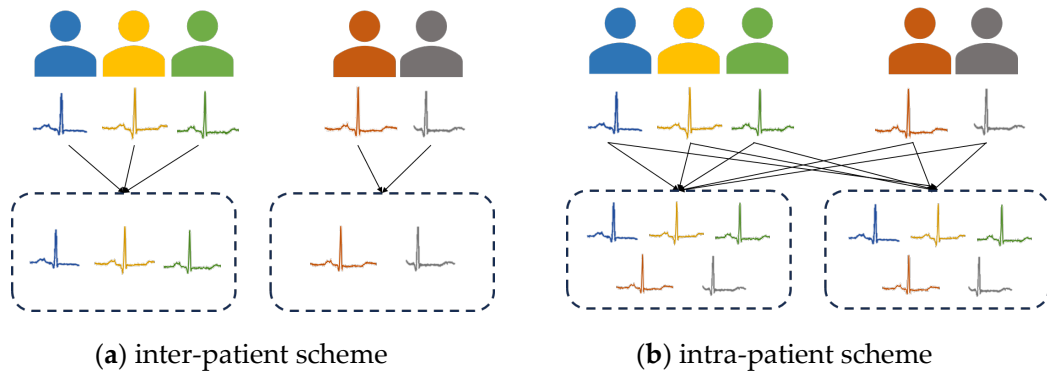


**Figure 1.** Illustration of (a) inter-patient scheme and (b) intra-patient scheme.

In this study, we introduce a novel subject-independent modeling approach for ECG-based arrhythmia classification that leverages our previous work on the n-BSM [10]. The n-BSM was originally suggested to efficiently classify ECG rhythms based on the beat-score maps (BSMs) without R-peak detection. The BSM is a 2D representation of the ECG signal aligned with detected R-peak positions. It consists of a chronological arrangement of beat-score vectors with zero interval paddings that capture beat-by-beat characteristics. The beat-score vectors are derived from a pre-trained beat classifier. The n-BSM is an improved version of the BSM that is generated by dividing a given ECG signal into  $n$  consecutive segments with a sliding window, thus eliminating the need for R-peak detection for ECG rhythm classification. The n-BSM image varies significantly across arrhythmia types, thereby allowing us to achieve superior performance in ECG-based arrhythmia classification. However, like other methods, the n-BSM also experiences a performance drop in inter-patient evaluation.

To alleviate the poor performance issue of the n-BSM-based approach within the patient-to-patient paradigm, we propose an adversarial framework to learn the characteristics of ECG signals, with a greater focus on beat-related features while eliminating patient-related features. We implemented this framework to make it applicable to the pre-training stage of the n-BSM beat classifier. Thus, a beat classifier pre-trained with an adversarial framework is used to generate beat-score vectors for a series of beat segments that make up a given ECG signal, followed by their chronological concatenation to form the corresponding n-BSM image. This resulting n-BSM is hereafter referred to as patient-independent BSM (PI-BSM). Utilizing the PI-BSM as an input to the arrhythmia rhythm classifier leads to improved classification performance compared to existing studies in the patient-to-patient paradigm. The contribution of our study is summarized as follows:

- The proposed method addresses inter-patient variability in ECG signals for the n-BSM-based arrhythmia classification by utilizing adversarial learning. Specifically, an adversarial framework is applied to the pre-training stage of the beat classifier used for PI-BSM generation. Consequently, PI-BSMs derived from ECG signals are able to effectively capture beat-related features while excluding patient-specific features;
- The proposed framework extends the applicability of the BSMs to cross databases by not mandating beat annotations. That is, a beat classifier can be pre-trained on any beat-annotated dataset (referred to as a source dataset), which is then used to derive PI-BSMs from other target datasets without beat annotations. This approach is suitable for real-world scenarios where beat annotations are lacking. Due to the enhanced generalization in the beat-level training phase, the PI-BSM can mitigate individual bias;

- The proposed method improves the performance of ECG arrhythmia classification in the inter-patient paradigm by using PI-BSMs as the input for a CNN-based rhythm classification model. Cross-validation within the MIT-BIH arrhythmia database (MIT-BIH dataset) showed a 14.27% improvement in the F1-score. When tested on the Chapman-Shaoxing 12-lead ECG database (SPH dataset) in a cross-database scenario, PI-BSM-based classification indicated a 4.97% improvement compared to our previous study;
- The proposed method achieves the most notable improvement in atrial fibrillation (AFib) rhythm, which exhibits the lowest performance in most other inter-patient studies. Utilizing this method demonstrated a 27.70% F1-score improvement in the MIT-BIH dataset cross-validation and a 16.22% increase in F1-score when tested with the SPH dataset. These findings confirm that there is significant variability among patients, particularly in AFib rhythms, and highlight the importance of taking this variability into account in AFib research.

## 2. Related Work

### 2.1. Subject-Specific Modeling Approach

To address the inter-subject variability in ECG signals, researchers have proposed subject-specific model approaches that fine-tune a general model for each individual patient.

Some studies utilize a constant portion of the ECG recording and its manual label from the test patient [11–16]. For example, researchers use the first 5 min of the test patient's ECG data to fine-tune the general model [11–13]. Li et al. [11] proposed a subject-specific model focusing on the usage of a wearable device. A preliminary generic CNN was initially trained using a large database in an off-device training phase and then fine-tuned using 5 min ECG signals obtained from individual patients in an on-device training phase. Xu et al. [12] transformed the initial 5 min ECG recording of the test patient into an identity vector, which was then injected into the intermediate layer of the general DNN model and fine-tuned by backpropagation. Instead of using the initial several minutes of the ECG recording, several studies select representative beats of the test patient, by employing the clustering technique [14] and active learning [15,16]. Despite some improvements in performance, these approaches require additional manual labeling, which is cost-expensive and impractical in real-world scenarios.

To avoid the need for expert labeling, recent studies have proposed automatic labeling methods [17–20]. Golany et al. [17] introduced the Personalized ECG Generative Adversarial Network (PGAN), which synthesizes ECG signals from an individual test patient. Zhai et al. [18,19] utilized estimated patient-specific normal beats by calculating the correlation coefficient between the spectrograms of the adjacent beats. The high-correlation beats are estimated as normal beats and are included in the fine-tuning dataset. Ye et al. [20] proposed a fusion model that combines a general model and a subject-specific model, where the subject-specific model utilizes multi-view learning to obtain high-confidence heartbeats from the subject's unlabeled initial 5 min ECG recording.

Despite the improvements in performance achieved by these subject-specific models, there are still some limitations that need to be addressed. Training a separate model for each individual can be time-consuming, and the automatic labeling methods used to generate pseudo-labels may not be entirely reliable, with the performance varying depending on the selected signals.

### 2.2. Subject-Independent Modeling Approach

In contrast to the subject-specific modeling approach, subject-independent models mitigate performance degradation in inter-patient schemes by expanding the model's generalization ability.

Niu et al. [21] developed a subject-independent model using a symbolization approach to minimize patient variations. They employ 1D ECG signals with RR intervals as inputs to the model, converting the symbolized ECG signals and RR intervals into embedded matrices, which are then concatenated to form the input to the classifier. To

obtain multi-perspective representations of distinct heartbeats, a multi-perspective CNN was used for classification. Xia et al. [22] introduced a subject-independent model that integrates a denoising autoencoder and a CNN with a lightweight transformer. They enhanced the performance of minority classes in the inter-patient scheme by extracting local features through the proposed seq2seq network and global features from adjacent heartbeats through a lightweight transformer encoder. Zhou et al. [23] proposed a CNN-based subject-independent model combining multi-scale convolution and frequency convolution block attention. They exhibited an improved ability to learn comprehensive features by leveraging convolution modules of varying sizes in the early layers. Guo et al. [24] proposed a hybrid model that combines two architectures. This model employs densely connected convolutional neural networks, gated recurrent unit networks, and attention mechanisms to capture the morphology and temporal differences of ECG beats to address inter-patient issues.

Several recent studies address inter-patient variability in ECG signals using domain adaptation techniques [25–28]. He et al. [25] propose a multi-level unsupervised domain adaptation framework that utilizes atrous spatial pyramid pooling residuals and a graph convolutional network model to extract the spatio-temporal structure and data-structure features, respectively. In the domain adaptation process, three types of alignment, namely domain alignment, semantic alignment, and structure alignment, are applied to reduce the gap between the source and target domains. Rafi and Ko [26] propose a source-free domain adaptation method for arrhythmia classification. This approach applies domain adaptation without requiring access to the source dataset by utilizing the local structure clustering method, which aligns target ECG features with similar neighbors. By not accessing the source dataset, this approach resolves data-privacy issues regarding patient information.

These subject-independent models offer the advantage of not requiring a separate fine-tuning process for each individual. However, the absence of a fine-tuning process may lead to the performance not being as high as subject-specific models. Despite the potential performance trade-off, using subject-independent models appears to be a more reasonable approach in real-world settings.

### 3. Materials and Methods

Figure 2 presents an overview of the proposed method, which consists of two phases, namely (a) beat-level training phase and (b) rhythm-level training phase. The first phase of beat-level training aims to pre-train a beat classifier using an adversarial framework to focus only on learning patient-independent features. The resulting beat classifier is referred to as the patient-independent beat classifier (PI-beat classifier). The PI-beat classifier is trained on 2.4 s ECG segments labeled with beat types, requiring an ECG dataset with beat annotations. Meanwhile, the second phase of rhythm-level training aims to train a rhythm classifier on 10 s ECG segments labeled with the arrhythmia type. The dataset utilized in each phase is referred to as the source dataset and the target dataset. More details on each phase are provided in Sections 3.2 and 3.3.

#### 3.1. Data Preprocessing

To ensure comparability with our previous study [10], the same preprocessing techniques and hyperparameter settings were employed. We utilized the discrete wavelet transform to eliminate the baseline drift and high-frequency noise from the 1D ECG signals. The decomposition scale was adjusted to 9 in Daubechies-4 (db4) to effectively remove baseline drift. To address high-frequency noise, the decomposition scale was set to 6, and frequencies ranging between 50 Hz and 100 kHz were filtered. Subsequently, the denoised ECG signals undergo segmentation using a window size of 2.4 s. This size was determined to ensure that it is large enough to include one beat cycle and its adjacent beat cycles. The 2.4 s ECG segments are then transformed into time-frequency images (scalograms) using continuous wavelet transform (CWT).

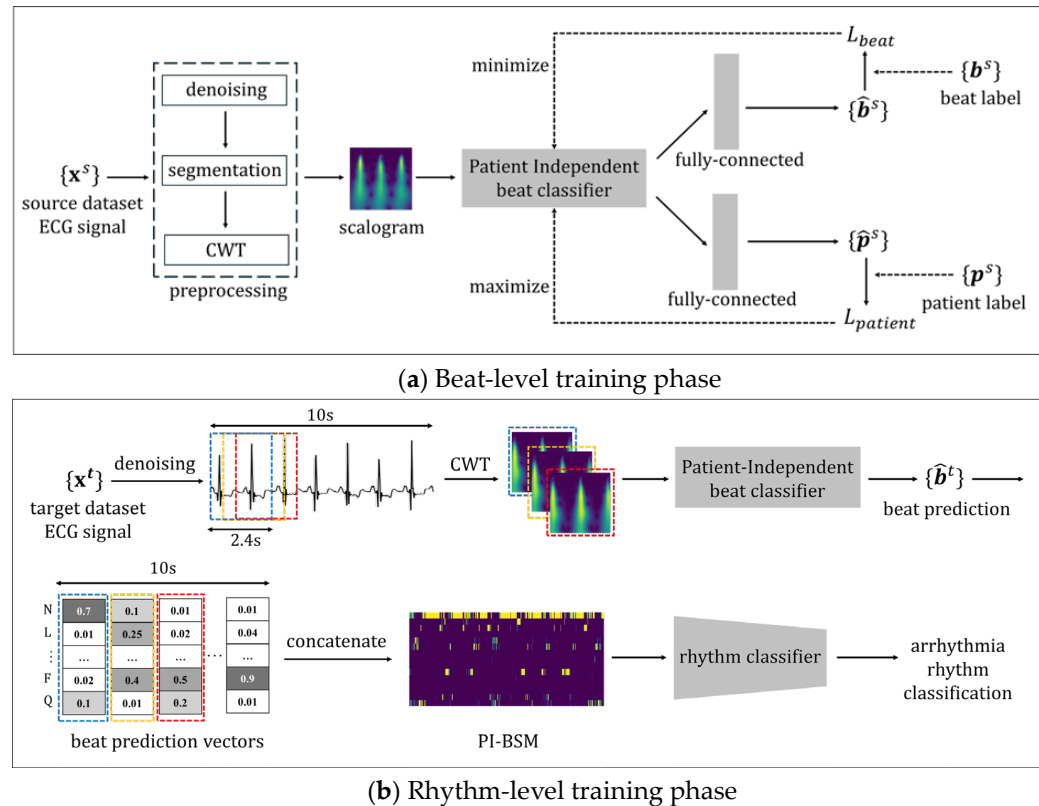


**Figure 2.** The overview of our proposed method. **(a)** In the beat-level training phase, we pre-train the patient-independent beat classifier. The classifier is trained using an adversarial framework to avoid learning patient-specific features of the ECG signal at the beat level. **(b)** In the rhythm-level training phase, beat-score vectors are generated using the pre-trained patient-independent beat classifier. These vectors are concatenated to generate a PI-BSM for a 10 s ECG signal, which serves as input to the rhythm classifier.

### 3.2. Beat-Level Training Phase

In the beat-level training phase, the PI-beat classifier is trained using a source dataset, denoted as  $D_s = \{(\mathbf{x}_i^s, \mathbf{b}_i^s, \mathbf{p}_i^s)\}_{i=1}^n$ , where  $n$  is the number of beat segment samples.  $\mathbf{x}_i^s$  denotes the  $i$ -th sample of a 2.4 s ECG segment (referred to as beat segment) labeled with a beat type  $\mathbf{b}_i^s$  for a patient with the identifier  $\mathbf{p}_i^s$ . The vectors  $\mathbf{b}^s$  and  $\mathbf{p}^s$  are represented as a one-hot encoding vector, each denoted as  $\mathbf{b}_i^s = [b_{i,1}, b_{i,2}, \dots, b_{i,B}]$  ( $B$ : the number of beat types) and  $\mathbf{p}_i^s = [p_{i,1}, p_{i,2}, \dots, p_{i,P}]$  ( $P$ : the number of patients), respectively.

Initially,  $\mathbf{x}^s$  undergoes the preprocessing step described in Section 3.1. The beat classifier is trained to capture the relationship between  $\mathbf{x}_i^s$  and  $\mathbf{b}_i^s$ , while disregarding the relationship between  $\mathbf{x}_i^s$  and  $\mathbf{p}_i^s$ . To realize this, we assume that the characteristics of the ECG beat segments can be split into beat-related features and patient-specific features. To take these features into account separately, we define two types of losses, namely beat-related loss ( $L_{beat}$ ) and patient-related loss ( $L_{patient}$ ). Ultimately, in our method, the model parameters are optimized to minimize  $L_{beat}$  while simultaneously maximizing  $L_{patient}$ .

#### Beat Loss ( $L_{beat}$ )

$L_{beat}$  is the loss to quantify the disparity between the predicted and actual beat classes and is calculated using the categorical cross-entropy, defined as:

$$L_{beat} = -\frac{1}{N} \sum_{i=1}^N \sum_{j=1}^B b_{i,j} \cdot \log(\hat{b}_{i,j}) \quad (1)$$

In Equation (1),  $N$  is the number of samples, and  $b_{i,j}$  and  $\hat{b}_{i,j}$  represent the ground-truth value and the prediction score for the  $i$ -th sample of the  $j$ -th beat class, respectively. By minimizing  $L_{beat}$  during training, the model can enhance its ability to predict beat classes.

#### Patient Loss ( $L_{patient}$ )

$L_{patient}$  is the loss to measure the discriminability between the predicted and actual patient labels. Since we intend to train the model so that it predicts patients poorly,  $L_{patient}$  needs to be maximized during training. To calculate  $L_{patient}$ , we utilized categorical cross-entropy, which is defined as:

$$L_{patient} = -\frac{1}{N} \sum_{i=1}^N \sum_{j=1}^P p_{i,j} \cdot \log(\hat{p}_{i,j}) \quad (2)$$

In Equation (2),  $N$  represents the total count of the samples.  $p_{i,j}$  denotes the ground truth, while  $\hat{p}_{i,j}$  signifies the prediction score of the  $i$ -th sample of the  $j$ -th patient ID.

#### Total Loss ( $L_{total}$ )

$L_{total}$  is defined as the weighted sum of  $L_{beat}$  and  $L_{patient}$ . The trade-off between beat classification ability and patient invariance needs to be carefully compromised to optimize the model parameters. To address this concern, the two losses are not assigned equal weights, and weighting coefficients  $\lambda_1$  and  $\lambda_2$  are introduced to  $L_{beat}$  and  $L_{patient}$ , respectively. Consequently,  $L_{total}$  is defined as:

$$L_{Total} = \lambda_1 \cdot L_{beat} - \lambda_2 \cdot L_{patient} \quad (3)$$

To train the PI-beat classifier, we employed a SE-ResNet model [29]. The SE-ResNet model combines the ResNet [30] architecture with a squeeze-and-excitation (SE) block. The SE block assigns varying weights to feature maps, emphasizing more crucial features to enhance performance. Considering its ability to suppress patient-related features, we deemed it appropriate to adopt SE-ResNet for inter-patient scenarios [31]. Figure 3 depicts the configuration of the PI-beat classifier.

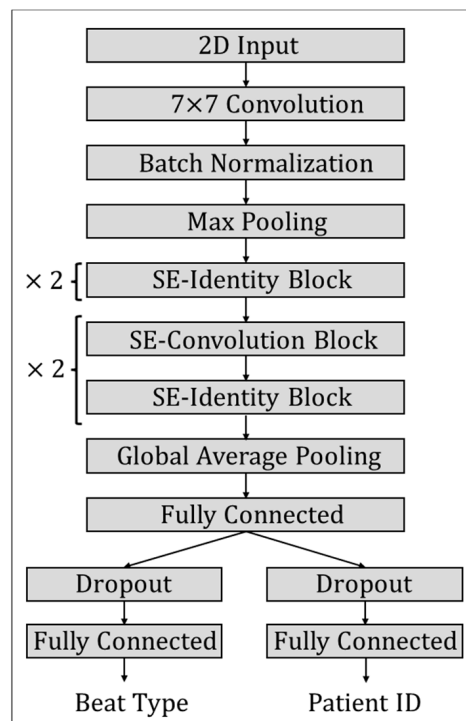


**Figure 3.** The overall architecture of the patient-independent beat classifier.

### 3.3. Rhythm-Level Training Phase

This section delves into the rhythm-level training phase, illustrated in Figure 2b. In this stage, the PI-BSM is generated, and the rhythm classifier is trained using PI-BSM as an input. We utilize a target dataset  $D_t = \{(\mathbf{x}_i^t, \mathbf{r}_i^t, \mathbf{p}_i^t)\}_{i=1}^m$ , where  $m$  represents the number of rhythm samples. The target dataset  $D_t$  comprises the 1D ECG signal  $\mathbf{x}_i^t$  with a duration of 10 s, along with corresponding rhythm annotations  $\mathbf{r}_i^t$  and patient identification label  $\mathbf{p}_i^t$ .  $\mathbf{x}_i^t$  is segmented with windows of size 2.4 s at intervals of 25 milliseconds, resulting in 360 beat segmentations for each 10 s  $\mathbf{x}_i^t$  sample. The segmented signal undergoes denoising and transformation into a 2D scalogram image using CWT.

Once the preprocessing stage is complete, scalogram images are fed into the pre-trained PI-beat classifier to generate  $d$ -dimensional beat-score vectors. Here,  $d$  is equal to the number of beat classes in the source data. Through the pre-trained PI-beat classifier, 360 beat-score vectors are generated for each  $\mathbf{x}_i^t$ . Arranging these beat-score vectors in chronological order produces a beat-score map, called the PI-BSM for a 10 s ECG signal.

Figure 4 illustrates the PI-BSMs for different rhythm types, where (a) represents AFib (atrial fibrillation), (b) GSVT (grouped supraventricular tachycardia), (c) SB (sinus Bradycardia), and (d) SR (sinus rhythm). The PI-BSMs for each rhythm type reflect reasonably well the distinct characteristics of ECG signals with different rhythm types. Table 1 provides a summary of the configuration of the rhythm classifier using SE-ResNet.

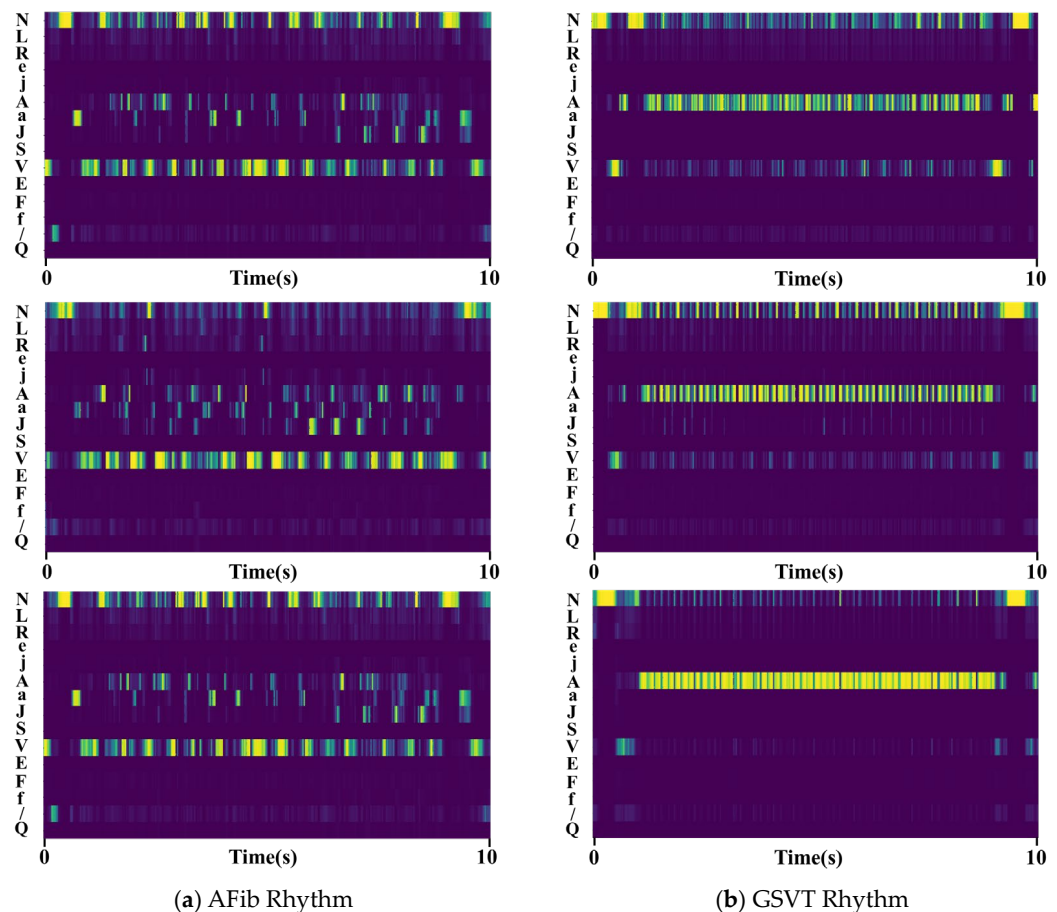


**Figure 4. Cont.**

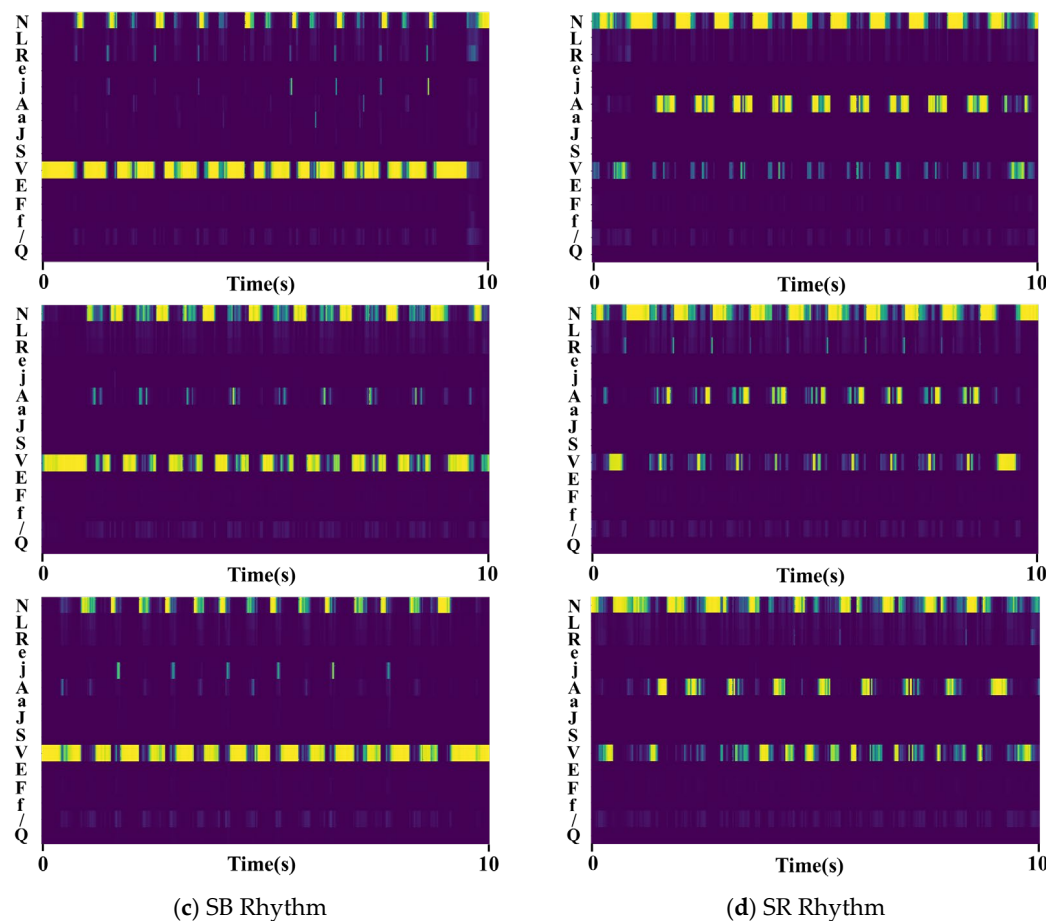


**Figure 4.** Examples of PI-BSM for various arrhythmia rhythm classes, exhibiting clear pattern distinctions.

**Table 1.** The architecture of the rhythm classifier.

Layer	Type	Output Size	Kernel Size	Strides
Layer 1	Inputs	(150 × 360 × 1)	7 × 7	2 × 2
Layer 2	2D Convolution layer	(75 × 180 × 64)	3 × 3	2 × 2
Layer 3	Max pooling	(37 × 89 × 64)	3 × 3	2 × 2
Layer 4	SE-Identity Block	(37 × 89 × 64)	3 × 3/5 × 5	1 × 1/1 × 1
Layer 5	SE-Identity Block	(37 × 89 × 64)	3 × 3/5 × 5	1 × 1/1 × 1
Layer 6	SE-Convolution Block	(19 × 45 × 128)	3 × 3/5 × 5/1 × 1	2 × 2/1 × 1/2 × 2
Layer 7	SE-Identity Block	(19 × 45 × 128)	3 × 3/5 × 5	1 × 1/1 × 1
Layer 8	SE-Convolution Block	(10 × 23 × 256)	3 × 3/5 × 5/1 × 1	2 × 2/1 × 1/2 × 2
Layer 9	SE-Identity Block	(10 × 23 × 256)	3 × 3/5 × 5	1 × 1/1 × 1
Layer 10	SE-Convolution Block	(5 × 12 × 512)	3 × 3/5 × 5/1 × 1	2 × 2/1 × 1/2 × 2
Layer 11	SE-Identity Block	(5 × 12 × 512)	3 × 3/5 × 5	1 × 1/1 × 1
Layer 12	Global Average Pooling	(512)	-	-

#### **4. Results and Discussion**

#### 4.1. Experimental Setup

### 4.1.1. Dataset

To evaluate the usability of the proposed method, we conducted experiments on two different public datasets, the MIT-BIH dataset and the SPH dataset.

The MIT-BIH dataset [32] consists of 48 records from 47 individuals. The database contains a 30 min, two-channel ECG recording with a sampling rate of 360 Hz. Each heartbeat is annotated at the R-peak, providing beat-level information. Additionally, arrhythmia rhythm annotations are provided at the rhythm level. In this study, we utilized the MLII lead among the two leads and incorporated both beat-level and rhythm-level annotations.

The SPH dataset [33] is a publicly available, large-scale ECG database. It comprises 12 lead recordings from 10,646 patients, each lasting 10 s, with a sampling rate of 500 Hz. Cardiologists have annotated each recording into 11 rhythm classes and 56 cardiovascular conditions. In this study, we used only lead II data and rhythm annotations to evaluate our algorithm.

#### 4.1.2. Hyperparameter Setting

For the SE-ResNet model used in the beat and rhythm classifier, we set the reduction ratio value to 16, since it achieves a good trade-off between accuracy and model complexity, as demonstrated in [29]. A batch size of 32 was configured, and the Adam optimizer was used with a learning rate of 0.00001.

#### 4.1.3. Evaluation Metrics

Precision, sensitivity, F1-score, and accuracy serve as evaluation metrics for our method. These criteria are defined as follows:

$$\text{Precision} = \frac{TP}{TP + FP} \quad (4)$$

$$\text{Sensitivity} = \frac{TP}{TP + FN} \quad (5)$$

$$\text{F1-score} = \frac{2 \times \text{Precision} \times \text{Sensitivity}}{\text{Precision} + \text{Sensitivity}} \quad (6)$$

$$\text{Accuracy} = \frac{TP + TN}{TP + TN + FP + FN} \quad (7)$$

Precision is the percentage of actual arrhythmia rhythms predicted as arrhythmias. Sensitivity is the percentage of actual arrhythmia rhythms predicted correctly. F1 score is the harmonic mean of the precision and the recall. Accuracy measures the percentage of rhythms tested that were correctly predicted, regardless of whether they were normal or arrhythmic.

#### 4.2. Experiment 1: Evaluation of the Proposed Method on a Single Database

To verify the effectiveness of the proposed method on a single database, experiments were performed using the MIT-BIH dataset. We used inter-patient recording divisions DS1 and DS2, as in [34], to evaluate the inter-patient performance. Table 2 illustrates the sample distribution of the 15 beat types in DS1 and DS2. Among these, only 11 common beats present in both DS1 and DS2 were utilized in this experiment.

**Table 2.** Number of beat samples in MIT-BIH DS1 and DS2.

	N	L	R	V	A	a	J	F
DS1	38041	3945	3776	3681	806	100	32	414
DS2	36386	4119	3472	3217	1734	50	514	388
j	E	Q	/	f	e	S	Record	
DS1	16	105	8	0	0	16	8	22
DS2	213	1	7	0	0	0	0	22

We utilized the DS2 dataset for the pre-training of the PI-beat classifier. To mitigate notable data imbalance in normal beats, we randomly sampled 20% of each patient's normal beats. The PI-beat classifier was trained to classify 11 types of beats and was used to generate PI-BSMs for 10 s ECG segments from DS1 and DS2. PI-BSMs were then fed into a binary rhythm classifier to distinguish AFib from normal rhythms. We took a binary classifier to alleviate the imbalance problem of rhythm labels. PI-BSMs from DS2 and DS1 were used for training and testing, respectively.

Figure 5 compares the baseline n-BSMs and PI-BSMs derived from identical 1D signals. The baseline n-BSM corresponds to our earlier work [10], where the adversarial framework

was not employed. Figure 5a showcases a normal rhythm, while (b) illustrates an AFib rhythm, each originating from different patients. In the PI-BSMs, the distinction between normal and AFib rhythms is observed more clearly than in the baseline n-BSMs. This is attributed to the exclusion of patient-specific features from both rhythms. In particular, the regular beat pattern becomes more evident for the normal rhythm, whereas the irregular pattern is emphasized in the AFib rhythm. Consequently, the PI-BSM results in a sharper contrast between the two rhythms than the baseline n-BSM.

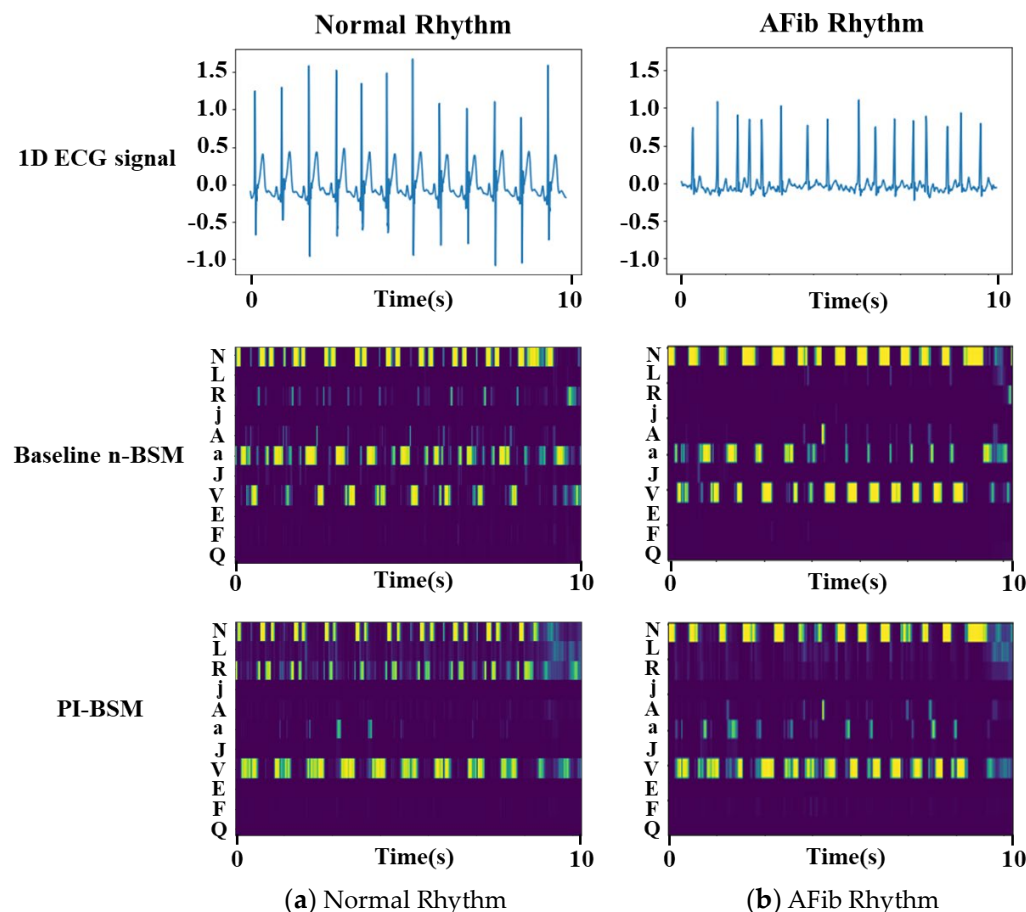


**Figure 5.** (a) depicts the normal rhythm, while (b) illustrates the AFib rhythm. The first row displays the 1D ECG signals derived from different patients in the MITBIH dataset. The second and third rows portray the baseline nBSM and PI-BSM transformed from each 1D ECG signal. The difference between normal and AFib rhythms may not be apparent in n-BSM images, but it becomes distinct in PIBSM images.

Figure 6a,b depict the confusion matrices when baseline n-BSM and PI-BSM are utilized as the input for rhythm classification, respectively. Table 3 compares precision, sensitivity, F1-score, and accuracy for the normal and AFib classes between baseline n-BSM and PI-BSM. These results show that PI-BSM exhibits a substantially improved performance compared to the baseline n-BSM. Specifically, there is a 4.94% increase for the normal rhythm and a 27.7% increase for AFib in the F1-score, highlighting the effectiveness of the adversarial framework when applied to n-BSM within a single database.

#### 4.3. Experiment 2: Evaluation of the Proposed Method on Cross-Database

In Experiment 2, we employed two distinct databases to verify the usability of the PI-BSM-based classification, particularly when the target dataset does not provide beat annotations. The MIT-BIH dataset was selected as the source dataset to use beat annotations, while the SPH dataset was chosen as the target dataset to classify arrhythmia rhythms. The PI-beat classifier was pre-trained to distinguish the 15 types of beats provided by the MIT-BIH dataset. The

target dataset ECG signal was converted to scalograms and input into the pre-trained PI-beat classifier to generate PI-BSM images, followed by classifying the rhythms.

Two preprocessing steps were additionally applied for the SPH dataset, namely missing-value exclusion and resampling. By conducting missing-value exclusion, only 10,588 samples were used in the analysis. Also, the ECG samples from the SPH dataset were resampled to 360 Hz to synchronize with the samples from the MIT-BIH dataset.

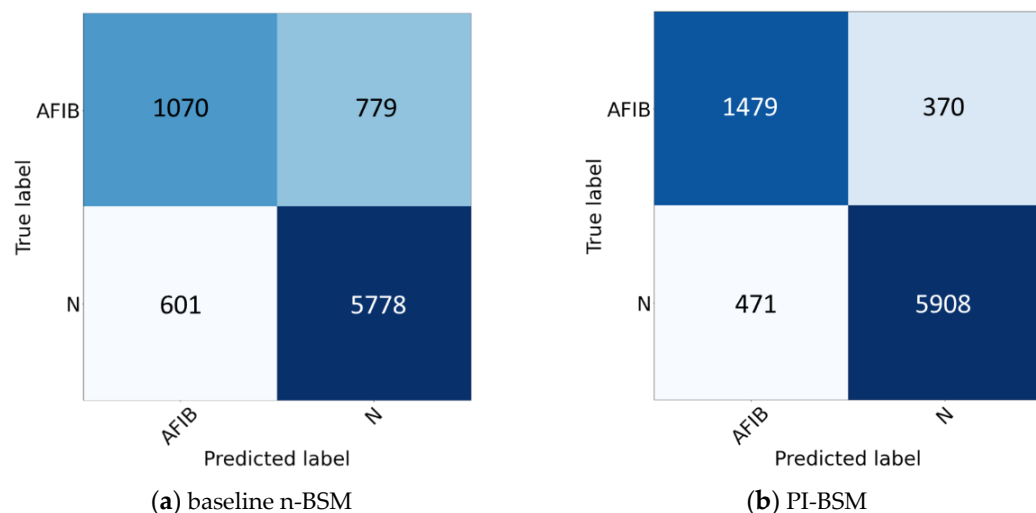


**Figure 6.** Confusion matrix of (a) baseline n-BSM and (b) PI-BSM using the MIT-BIH dataset.

In Table 4, the number and types of samples in the SPH dataset are presented, both before and after preprocessing. Several rhythms have a limited quantity of data, which is unsuitable for training a deep-learning model. To address the data imbalance problem, the original 11 rhythm types were merged and created into 4 different rhythm types (AFib, GSVT, SB, and SR) based on the guidelines [33]. As all samples in the SPH dataset were from different patients, dataset partitioning was performed without considering patient labels, and 5-fold cross-validation was used for inter-patient evaluation.

**Table 3.** Performance comparison with previous studies and our proposed method in the MIT-BIH dataset.

	Normal Rhythm			AFib Rhythm			Overall	
	Pre	Sen	F1	Pre	Sen	F1	F1	Acc
Baseline	87.7	90.3	89.0	64.0	57.9	61.0	75.0	83.2
PI-BSM	94.1	92.6	93.4	75.8	80.0	77.9	85.7	89.8

**Table 4.** Number of samples in SPH dataset before and after preprocessing.

Merged Rhythm	Rhythm	Number of Samples		
		Before Preprocessing		After Preprocessing
AFIB	Atrial Flutter	445	2225	438
	Atrial Fibrillation	1780		1780
	Atrial Tachycardia	121		121
	Atrioventricular Node Reentrant Tachycardia	16		16
GSVT	Atrioventricular Reentrant Tachycardia	8	2307	8
	Sinus Atrium to Atrial Wandering Rhythm	7		7

**Table 4.** Cont.

Merged Rhythm	Rhythm	Number of Samples	
		Before Preprocessing	After Preprocessing
GSVT	Sinus Tachycardia	1568	1564
	Supraventricular Tachycardia	587	2307
SB	Sinus Bradycardia	3889	3889
	Sinus Rhythm	1836	2225
SR	Sinus Irregularity	399	1564
	Total	10,646	2222
		397	20,588

In the subsequent subsections, we performed three analyses. Section 4.3.1 examines the impact of patient loss ( $L_{patient}$ ) on PI-PSM generation. Section 4.3.2 investigates the influence of PI-BSM in cross-domain scenarios. Section 4.3.3 compares the performance with other state-of-the-art methods.

#### 4.3.1. Effect of Patient Loss ( $L_{patient}$ ) on PI-BSM Generation

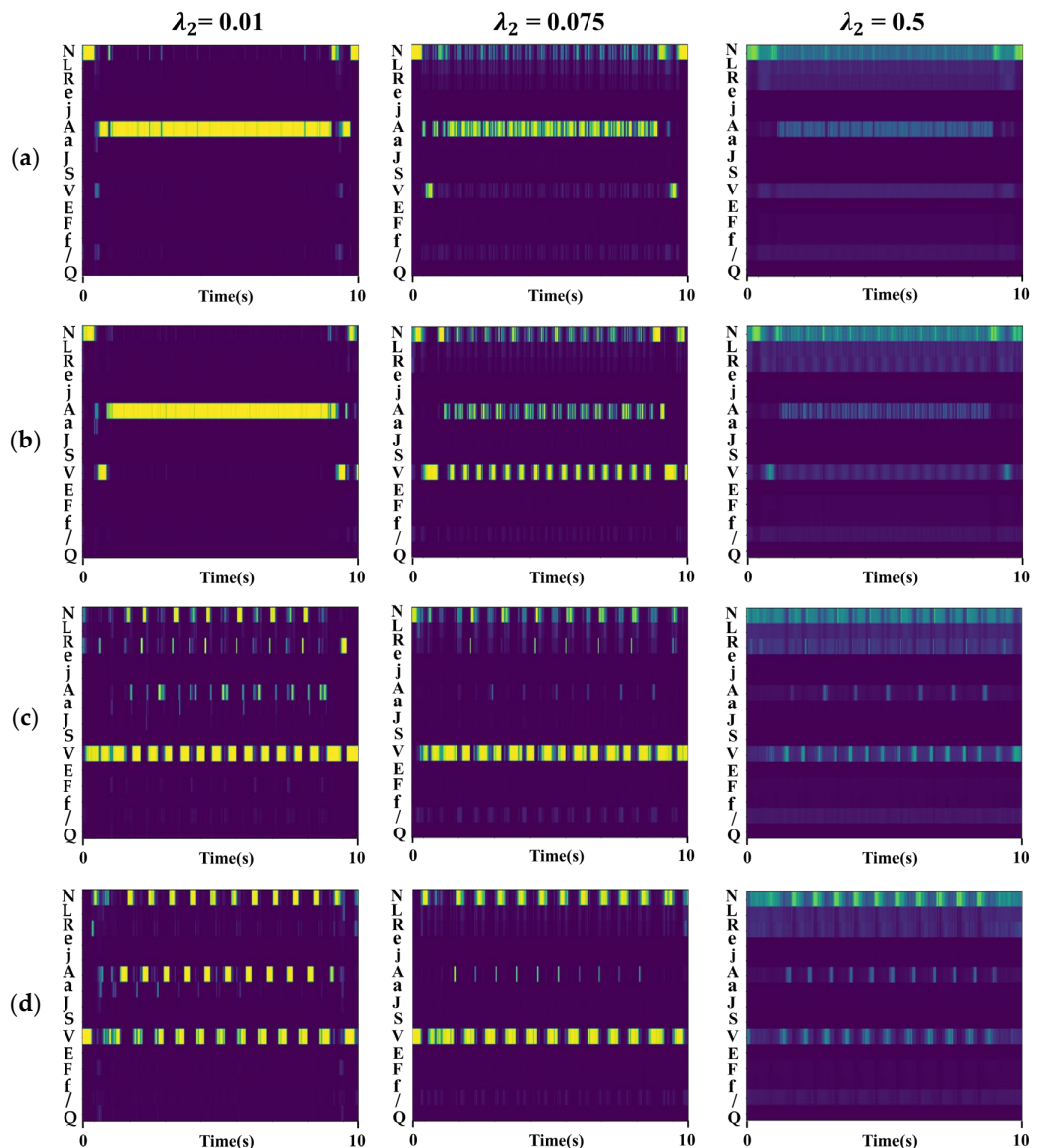
In this section, we conducted experiments to analyze the impact of patient loss ( $L_{patient}$ ), described in Equation (3), on PI-BSM generation. In this equation, the hyperparameter  $\lambda_2$  serves to control the degree to which patient loss is reflected in the PI-beat-classifier training, with  $\lambda_1$  being fixed at one. Increasing the value of  $\lambda_2$  results in less learning of patient-specific features, thereby increasing the patient invariance of the model. On the other hand, decreasing the value of  $\lambda_2$  enlarges learning about patient-specific features and reduces patient invariance in the model.

Figure 7 depicts PI-BSM images of four different rhythm samples generated using different  $\lambda_2$  values of 0.01, 0.075, and 0.5, where (a), (b), (c), and (d) represent the AFib, GSVT, SB, and SR rhythms, respectively. This illustrates that the value of  $\lambda_2$  highly influences the pattern of PI-BSM. When  $\lambda_2$  is set to 0.5, the image appears blurry, making it difficult to distinguish between the 15 beat types. This is attributed to relatively little learning of beat-related characteristics from ECG signals in the PI-beat-classifier training stage. Conversely, setting  $\lambda_2$  to 0.01 removes patient-specific features less, making the PI-BSM images less discriminative across rhythm types. Table 5 compares the performance of rhythm classification for different  $\lambda_2$  values. Based on Table 5 and Figure 7, 0.075 was chosen as the optimal weight for the SPH dataset. For subsequent experiments, the hyperparameter was, thus, fixed at 0.075.

From Table 5, it is observed that AFib exhibited the lowest performance in the baseline setting but improved by 16.22% through the proposed framework, marking the most substantial enhancement among the four rhythms evaluated. These results demonstrate that significant variability exists among patients with AFib rhythm, decreasing performance in inter-patient schemes. Thus, the elimination of patient variability appears to be crucial for accurate AFib detection.

**Table 5.** Performance comparison for different hyperparameters  $\lambda_2$  in the SPH dataset.

Parameter $\lambda_2$	AFIB <sub>F1</sub> (%)	GSVT <sub>F1</sub> (%)	SB <sub>F1</sub> (%)	SR <sub>F1</sub> (%)	Avg <sub>F1</sub> (%)	Acc (%)
baseline	67.43	84.04	95.34	86.08	83.22	86.29
$\lambda_2 = 0.01$	73.86	85.09	96.01	88.10	85.77	87.56
$\lambda_2 = 0.05$	71.07	82.69	95.77	85.85	83.85	85.90
$\lambda_2 = 0.075$	78.37	86.87	95.88	88.32	87.36	88.73
$\lambda_2 = 0.1$	76.81	86.98	96.90	87.59	87.07	88.71
$\lambda_2 = 0.25$	75.45	86.24	94.57	86.52	85.69	87.24
$\lambda_2 = 0.5$	76.16	86.40	95.75	86.98	86.32	87.82



**Figure 7.** PI-BSM images varying with different hyperparameters  $\lambda_2$  are shown in (a) for AFIB, (b) for GSVT, (c) for SB, and (d) for SR.

#### 4.3.2. Characterization of PI-BSMs through Adversarial Learning

Figure 8 showcases the baseline n-BSM and PI-BSM images derived from the AFib ECG signals of distinct patients in the SPH dataset. For the same AFib rhythm, three baseline n-BSM images exhibit contrasting patterns, making it challenging to discern an identical rhythm type. In contrast, the PI-BSM images exhibit stronger similarity between the same AFib rhythm samples. This is due to the amplitude variation in the 1D signals among patients, even for the same AFib rhythm, as illustrated in Figure 8. Therefore, the beat-score vectors generated to form the baseline n-BSM show varying beat predictions by each patient, leading to a failure to capture shared information for AFib rhythms. Unlike n-BSMs, the proposed method using PI-BSMs enables focusing on learning the beat characteristics while excluding the individual characteristics by adversarial learning. As a result, it has become possible to clearly distinguish between different ECG rhythms by leveraging shared information about the same rhythm across patients.

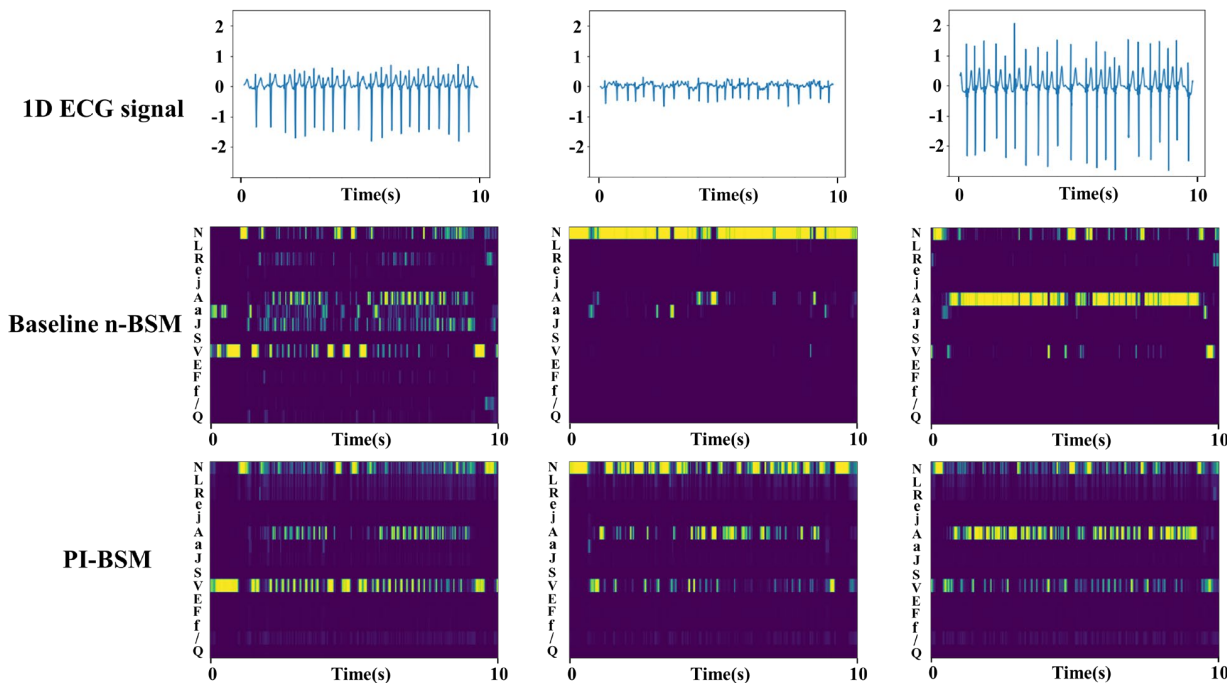


**Figure 8.** The first row consists of AFib patient’s 1D ECG signals derived from three different patients in the SPH dataset. The second and third rows depict the baseline n-BSMs and PI-BSMs transformed from the 1D ECG signals. PI-BSM images show more similarity than 1D ECG signals or baseline n-BSM.

#### 4.3.3. Comparison with State-of-the-Art Methods

Table 6 summarizes recent studies on classifying arrhythmia rhythms using ECG signals. The PhysioNet 2017 challenge dataset, which evaluates the model’s inter-patient scenario, has been employed in various studies. Chandra et al. [35] and Andreotti et al. [36] used this dataset to classify arrhythmia rhythms, achieving an F1 score of 83.0% using ResNet and achieving 71.0% with CNN, respectively.

When considering multiple datasets utilization for training, our method shows promising results. Aziz et al. [37] showed that, when incorporating the MIT-BIH and SPH datasets into training, the F1 score substantially dropped to 60.3% compared to 89.5% when utilizing the SPH dataset alone. Zhang et al. [38] used 12 leads with the two datasets, and this performed slightly better than our proposed method. However, no significant enhancement was seen even when using an additional 11 leads for rhythm classification.

Our proposed method outperforms other studies that utilize a single lead and multiple datasets in inter-patient evaluation, achieving the highest F1 score of 87.4%. This is due to our approach’s consideration of patient-dependent features in ECG signals and the application of adversarial learning to exclude these features during the beat classifier training process, unlike in other studies [37,38]. By focusing more on beat-related features during beat-classifier training, our method demonstrates superior performance in arrhythmia classification in the inter-patient scheme.

**Table 6.** Comparison of classification performance with the state-of-the-art methods.

Authors	Database	No. of Classes	Method	Evaluation	Lead	F1-Score	Accuracy
Chandra et al. [35] (2017)	PhysioNet 2017	3	CNN	Inter-patient	1	71.0	Unknown
Andreotti et al. [36] (2017)	PhysioNet 2017	3	ResNet	Inter-patient	1	83.0	Unknown

**Table 6.** Cont.

Authors	Database	No. of Classes	Method	Evaluation	Lead	F1-Score	Accuracy
Murat et al. [39] (2021)	SPH	4	Hybrid DNN	Intra-patient	1	97.7	98.0
Aziz et al. [37] (2021)	SPH	4	MLP	Unknown	1	89.5	90.7
Aziz et al. [37] (2021)	MIT-BIH, SPH	3	MLP	Unknown	1	60.3	68.0
Zhang et al. [38] (2023)	NFH, SPH	4	ST-ReGE	Inter-patient	12	88.0	89.7
Lee et al. [10] (2024)	MIT-BIH, SPH	4	SE-ResNet	Inter-patient	1	83.2	86.3
Proposed Method	MIT-BIH, SPH	4	SE-ResNet	Inter-patient	1	87.4	88.7

## 5. Conclusions

Despite the widespread application of deep-learning-based diagnostic models for ECG rhythm classification, the challenge of individual variability of ECGs remains. This inter-variability leads to decreased performance when dealing with unseen patients in real-world scenarios.

In this study, we addressed the performance-degradation issue encountered in the inter-patient scheme, particularly when using an n-BSM-based ECG rhythm classification. Given the significant variability of ECG signals across individuals, it is essential to minimize the impact of this variability on arrhythmia classification. To address this problem, we introduced the PI-BSM-based classification framework, which leverages adversarial learning to eliminate patient-specific characteristics during the training of the beat classifier used for PI-BSM generation.

We conducted PI-BSM experiments in both single-database and cross-database scenarios within a patient-to-patient framework. Our framework demonstrated significant improvements in ECG rhythm classification compared to the original n-BSM approach. Notably, it showed enhanced performance in detecting abnormal rhythms, such as AFib, where cross-patient evaluations suffer from significant performance decline.

For real-world medical applications, the patient's ECG signal (10 s or longer in length) needs to be recorded and converted into a PI-BSM image by a pre-trained beat classifier. This beat classifier can be pre-trained on any available large-scale ECG database with good-quality beat annotations. However, for more reliable results, additional processing, such as domain adaptation, may be required while training the beat classifier. With a good pre-trained beat classifier, our method can easily generate PI-BSM from the provided ECG signal and use it for rhythm classification. No additional online training process is required.

Nevertheless, there is still room for further improvement in classification performance, especially in cross-database scenarios. Future research will focus on exploring domain adaptation techniques for the beat classifier to enhance performance in classifying arrhythmia rhythms using PI-BSM across different databases.

**Author Contributions:** Conceptualization, Y.J.; methodology, M.S.; formal analysis, Y.J.; investigation, J.L.; data curation, Y.J. and J.L.; writing—original draft preparation, Y.J.; writing—review and editing, M.S. and J.L.; visualization, Y.J.; supervision, M.S.; project administration, M.S.; funding acquisition, M.S. All authors have read and agreed to the published version of the manuscript.

**Funding:** This work was mainly supported by the Basic Science Research Program through the National Research Foundation of Korea (NRF) funded by the Ministry of Education (2022R1I1A3054343). Also, this work was partly supported by the Commercialization Promotion Agency for R&D Outcomes (COMPA) grant funded by the Korean Government (Ministry of Science and ICT) (RS-2023-00304695).

**Institutional Review Board Statement:** Not applicable.

**Informed Consent Statement:** Not applicable.

**Data Availability Statement:** The data presented in this study are openly available in PhysioNet at <https://physionet.org/content/mitdb/1.0.0/> (accessed on 13 November 2023), reference number [32] and <https://physionet.org/content/ecg-arrhythmia/1.0.0/> (accessed on 5 December 2023), reference number [33].

**Conflicts of Interest:** The authors declare no conflicts of interest.

## Abbreviations

The following abbreviations are used in this manuscript:

N	normal beat
L	left bundle branch block beat
R	right bundle branch block beat
A	atrial premature beat
a	aberrated atrial premature beat
J	junctional premature beat
S	supraventricular premature beat
V	premature ventricular contraction
F	fusion of ventricular and normal beat
e	atrial escape beat
j	junctional escape beat
E	ventricular escape beat
/	paced beat
f	fusion of paced and normal beat
Q	unclassifiable beat
AFib	atrial fibrillation
GSVT	grouped supraventricular tachycardia
SR	sinus rhythm
SB	sinus bradycardia

## References

1. Murat, F.; Yildirim, O.; Talo, M.; Baloglu, U.; Demir, Y.; Acharya, U. Application of deep learning techniques for heartbeats detection using ECG signals-analysis and review. *Comput. Biol. Med.* **2020**, *120*, 103726. [[CrossRef](#)] [[PubMed](#)]
2. Haugaa, K.H.; Edvardsen, T.; Amlie, J.P. Prediction of life-threatening arrhythmias—still an unresolved problem. *Cardiology* **2011**, *118*, 129–137. [[CrossRef](#)] [[PubMed](#)]
3. Berger, F.A.; Sijs, H.; Gelder, T.; Kuijper, A.F.; Bemt, P.M.; Becker, M.L. Comparison of two algorithms to support medication surveillance for drug-drug interactions between QTc-prolonging drugs. *Int. J. Med. Inform.* **2021**, *145*, 104329. [[CrossRef](#)] [[PubMed](#)]
4. Sinal, M.S.; Kamioka, E. Early abnormal heartbeat multistage classification by using decision tree and K-nearest neighbor. In Proceedings of the 2018 Artificial Intelligence and Cloud Computing Conference, New York, NY, USA, 21–23 December 2018; pp. 29–34. [[CrossRef](#)]
5. Saber, M.; Abotaleb, M. Arrhythmia modern classification techniques: A review. *J. Artif. Intell. Metaheuristics* **2022**, *1*, 42–53. [[CrossRef](#)]
6. Xiao, Q.; Lee, K.; Mokhtar, S.A.; Ismail, I.; Pauzi, A.L.B.M.; Zhang, Q.; Lim, P.Y. Deep learning-based ECG arrhythmia classification: A systematic review. *Appl. Sci.* **2023**, *13*, 4964. [[CrossRef](#)]
7. Liu, W.; Huang, Q.; Chang, S.; Wang, H.; He, J. Multiple-feature-branch convolutional neural network for myocardial infarction diagnosis using electrocardiogram. *Biomed. Signal Process. Control* **2018**, *45*, 22–32. [[CrossRef](#)]
8. Xu, S.S.; Mak, M.W.; Chang, C. Inter-patient ECG classification with i-vector based unsupervised patient adaptation. *Expert Syst. Appl.* **2022**, *210*, 118410. [[CrossRef](#)]
9. Zahid, M.U.; Kiranyaz, S.; Gabbouj, M. Global ECG classification by self-operational neural networks with feature injection. *IEEE Trans. Biomed. Eng.* **2022**, *70*, 205–215. [[CrossRef](#)] [[PubMed](#)]
10. Lee, J.; Shin, M. Using beat score maps with successive segmentation for ECG classification without R-peak detection. *Biomed. Signal Process. Control* **2024**, *91*, 105982. [[CrossRef](#)]
11. Li, Y.; Pang, Y.; Wang, J.; Li, X. Patient-specific ECG classification by deeper CNN from generic to dedicated. *Neurocomputing* **2018**, *314*, 336–346. [[CrossRef](#)]
12. Xu, S.S.; Mak, M.W.; Cheung, C.C. I-vector-based patient adaptation of deep neural networks for 22 automatic heartbeat classification. *IEEE J. Biomed. Health Inform.* **2019**, *24*, 717–727. [[CrossRef](#)] [[PubMed](#)]
13. Kiranyaz, S.; Ince, T.; Gabbouj, M. Real-time patient-specific ECG classification by 1-D convolutional neural networks. *IEEE Trans. Biomed. Eng.* **2015**, *63*, 664–675. [[CrossRef](#)] [[PubMed](#)]

14. Zhang, C.; Wang, G.; Zhao, J.; Gao, P.; Lin, J.; Yang, H. Patient-specific ECG classification based on recurrent neural networks and clustering technique. In Proceedings of the 2017 13th IASTED International Conference on Biomedical Engineering (BioMed), Innsbruck, Austria, 20–21 February 2017; pp. 63–67. [[CrossRef](#)]
15. Xia, Y.; Zhang, H.; Xu, L.; Gao, Z.; Zhang, H.; Liu, H.; Li, S. An automatic cardiac arrhythmia classification system with wearable electrocardiogram. *IEEE Access* **2018**, *6*, 16529–16538. [[CrossRef](#)]
16. Rahhal, M.M.; Bazi, Y.; AlHichri, H.; Alajlan, N.; Melgani, F.; Yager, R.R. Deep learning approach for active classification of electrocardiogram signals. *Inf. Sci.* **2016**, *345*, 340–354. [[CrossRef](#)]
17. Golany, T.; Radinsky, K. Pgans: Personalized generative adversarial networks for ecg synthesis to improve patient-specific deep ecg classification. In Proceedings of the AAAI Conference on Artificial Intelligence, Honolulu, HI, USA, 27 January–1 February 2019; Volume 33, pp. 557–564. [[CrossRef](#)]
18. Zhai, X.; Zhou, Z.; Tin, C. Semi-supervised learning for ECG classification without patient-specific labeled data. *Expert Syst. Appl.* **2020**, *158*, 113411. [[CrossRef](#)]
19. Zhou, Z.; Zhai, X.; Tin, C. Fully automatic electrocardiogram classification system based on generative adversarial network with auxiliary classifier. *Expert Syst. Appl.* **2021**, *174*, 114809. [[CrossRef](#)]
20. Ye, C.; Kumar, B.V.K.V.; Coimbra, M.T. An automatic subject-adaptable heartbeat classifier based on multiview learning. *IEEE J. Biomed. Health Inform.* **2015**, *20*, 1485–1492. [[CrossRef](#)] [[PubMed](#)]
21. Niu, J.; Tang, Y.; Sun, Z.; Zhang, W. Inter-patient ECG classification with symbolic representations and multi-perspective convolutional neural networks. *IEEE J. Biomed. Health Inform.* **2019**, *24*, 1321–1332. [[CrossRef](#)] [[PubMed](#)]
22. Xia, Y.; Xiong, Y.; Wang, K. A transformer model blended with CNN and denoising autoencoder for inter-patient ECG arrhythmia classification. *Biomed. Signal Process. Control* **2023**, *86*, 105271. [[CrossRef](#)]
23. Zhou, F.; Sun, Y.; Wang, Y. Inter-patient ECG arrhythmia heartbeat classification network based on multiscale convolution and FCBA. *Biomed. Signal Process. Control* **2024**, *90*, 105789. [[CrossRef](#)]
24. Guo, L.; Sim, G.; Matuszewski, B. Inter-patient ECG classification with convolutional and recurrent neural networks. *Biocybern. Biomed. Eng.* **2019**, *39*, 868–879. [[CrossRef](#)]
25. He, Z.; Chen, Y.; Yuan, S.; Zhao, J.; Yuan, Z.; Polat, K.; Alhudhaif, A.; Alenezi, F.; Hamid, A. A novel unsupervised domain adaptation framework based on graph convolutional network and multi-level feature alignment for inter-subject ECG classification. *Expert Syst. Appl.* **2023**, *221*, 119711. [[CrossRef](#)]
26. Rafi, T.H.; Ko, Y. SF-ECG: Source-free intersubject domain adaptation for electrocardiography-based arrhythmia classification. *Appl. Sci.* **2023**, *13*, 8551. [[CrossRef](#)]
27. Yuan, L.; Siyal, M.Y. Target-oriented augmentation privacy-protection domain adaptation for imbalanced ECG beat classification. *Biomed. Signal Process. Control* **2023**, *86*, 105308. [[CrossRef](#)]
28. Feng, P.; Fu, J.; Ge, Z.; Wang, H.; Zhou, Y.; Zhou, B.; Wang, Z. Unsupervised semantic-aware adaptive feature fusion network for arrhythmia detection. *Inf. Sci.* **2022**, *582*, 509–528. [[CrossRef](#)]
29. Hu, J.; Shen, L.; Sun, G. Squeeze-and-excitation networks. In Proceedings of the IEEE Conference on Computer Vision and Pattern Recognition, Salt Lake City, UT, USA, 18–23 June 2018; pp. 7132–7141.
30. He, K.; Zhang, X.; Ren, S.; Sun, J. Deep residual learning for image recognition. In Proceedings of the IEEE Conference on Computer Vision and Pattern Recognition, Las Vegas, NV, USA, 27–30 June 2016; pp. 770–778.
31. Wang, G.; Chen, M.; Ding, Z.; Li, J.; Yang, H.; Zhang, P. Inter-patient ECG arrhythmia heartbeat classification based on unsupervised domain adaptation. *Neurocomputing* **2021**, *454*, 339–349. [[CrossRef](#)]
32. Moody, G.B.; Mark, R.G. The impact of the MIT-BIH arrhythmia database. *IEEE Eng. Med. Biol. Mag.* **2001**, *20*, 45–50. [[CrossRef](#)] [[PubMed](#)]
33. Zheng, J.; Zhang, J.; Danioko, S.; Yao, H.; Guo, H.; Rakovski, C. A 12-lead electrocardiogram database for arrhythmia research covering more than 10,000 patients. *Sci. Data* **2020**, *7*, 48. [[CrossRef](#)] [[PubMed](#)]
34. Chazal, P.; O'Dwyer, M.; Reilly, R.B. Automatic classification of heartbeats using ECG morphology and heartbeat interval features. *IEEE Trans. Biomed. Eng.* **2004**, *51*, 1196–1206. [[CrossRef](#)] [[PubMed](#)]
35. Chandra, B.S.; Sastry, C.S.; Jana, S.; Patidar, S. Atrial fibrillation detection using convolutional neural networks. In Proceedings of the 2017 Computing in Cardiology (CINC), Rennes, France, 24–27 September 2017. [[CrossRef](#)]
36. Andreotti, F.; Carr, O.; Pimentel, M.A.; Mahdi, A.; De Vos, M. Comparing feature-based classifiers and convolutional neural networks to detect arrhythmia from short segments of ECG. In Proceedings of the 2017 Computing in Cardiology (CINC), Rennes, France, 24–27 September 2017. [[CrossRef](#)]
37. Aziz, S.; Ahmed, S.; Alouini, M.S. ECG-based machine-learning algorithms for heartbeat classification. *Sci. Rep.* **2021**, *11*, 18738. [[CrossRef](#)] [[PubMed](#)]
38. Zhang, H.; Liu, W.; Chang, S.; Wang, H.; He, J.; Huang, Q. ST-ReGE: A Novel Spatial-Temporal Residual Graph Convolutional Network for CVD. *IEEE J. Biomed. Health Inform.* **2023**, *28*, 216–227. [[CrossRef](#)]
39. Murat, F.; Yildirim, O.; Talo, M.; Demir, Y.; Tan, R.S.; Ciaccio, E.J.; Acharya, U.R. Exploring deep features and ECG 23 attributes to detect cardiac rhythm classes. *Knowl. Based Syst.* **2021**, *232*, 107473. [[CrossRef](#)]